JOC The Journal of Organic Chemistry

Note

pubs.acs.org/joc

Radical Cation of an Oligoarylamine Having a Nitroxide Radical Substituent: A Coexistent Molecular System of Localized and Delocalized Spins

Akihiro Ito,* Ryohei Kurata, Yusuke Noma, Yasukazu Hirao,† and Kazuyoshi Tanaka

Department of Molecular Engineering, Graduate School of Engineering, Kyoto University, Nishikyo-ku, Kyoto 615-8510, Japan

Supporting Information

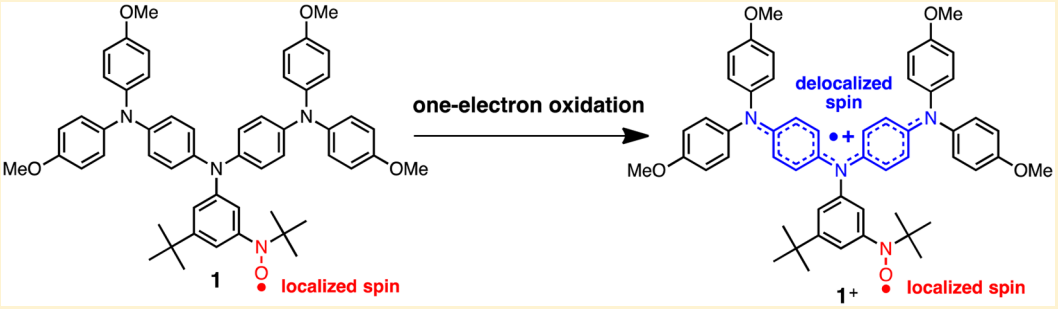

ABSTRACT: A trimer derivative of oligotriarylamine bearing a nitroxide radical substituent as a localized spin center {*N*,*N*-bis[4-(di-4-anisylamino)phenyl]-*N*-[3-*tert*-butyl-5-(*N*-*tert*-butyl-*N*-oxylamino)phenyl]amine (**1**)} was characterized by electrochemical, spectroelectrochemical, and electron paramagnetic resonance spectroscopic measurements. The first and second oxidations of **1** occurred from the triamine moiety, leaving the nitroxide radical moiety intact. The delocalized polaronic state in the triamine moiety was generated by one-electron oxidation of **1**, indicating the coexistence of localized and delocalized spins on $\mathbf{1}^{+}$, where an intramolecular antiferromagnetic interaction was detected.

Interplay between localized and delocalized spins in multispin organic molecular systems is of great interest for the realization of molecule-based spin electronics.[1] In particular, spin transport properties based on organic spin filters are being theoretically examined.[2] Previous theoretical study in our group has shown that the ferromagnetic coupling between the localized and delocalized spins gives rise to the spin-polarized state.[3] On the basis of this prediction, we confirmed that the parallel spin alignment between localized spins was mediated by a delocalized spin in multispin organic molecular systems.[4] In addition, if the charge distribution and/or intramolecular charge transfer of the delocalized spins originating from the charged moieties in the multispin molecular systems can be controlled by the interaction with the localized spins, such coexistent molecular systems of localized and delocalized spins are of great interest in conjunction with the control of spin transport properties.[1]

As for the organic radical ions possessing the delocalized spin, extensive studies of the nature of the intervalence (IV) states in the partially oxidized states of oligoarylamines have been conducted.[5] The arylamines can be recognized as useful redox-active molecular units because of the stability of their oxidized states,[6−8] and therefore, they play a pivotal role in various applications such as organic solar cell (OSC) dyes,[9] thermally activated delayed fluorescence dyes for organic light-emitting diodes (OLED),[10] etc. Generally, two (or more) equivalent redox-active units are connected by proper bridging units such as *p*-phenylene, and the delocalized IV state can be generated in the partially oxidized (or reduced) states. For instance, the charge (or spin) delocalization over the three redox-active amine units in the radical cation of triamine **2** has been demonstrated by spectroscopic methods,[6] and thus, such a charge-delocalized state can be considered as a suitable model for polaronic states generated by p-type doping of *N*-phenyl-substituted polyaniline (Figure 1a).[11]

Herein, we report on the electronic structures of oligoarylamine **1**, in which the nitroxide radical group is substituted in the central N position of triamine **2** as a localized spin center.[12] In particular, the electronic structures of the oxidized species, $\mathbf{1}^{+}$ and $\mathbf{1}^{2+}$, were examined as multispin molecular systems in which localized and delocalized spins are coexistent. Diradical cation $\mathbf{1}^{+}$ can be regarded as a minimal model compound for realizing the spin-polarized molecular wires, when an intramolecular magnetic interaction exists between the localized and delocalized spins (Figure 1b).[1,3,4] Such heterogeneous multispin molecular systems based on the so-called redox modulation of the intramolecular magnetic coupling among the localized spin centers have attracted attention in the past few years.[13]

Nitroxide-substituted triamine **1** was prepared by Ag_2O oxidation after deprotection of compound **5**, which was

Received: August 21, 2016
Published: November 1, 2016

DOI: 10.1021/acs.joc.6b02037
J. Org. Chem. 2016, 81, 11416−11420

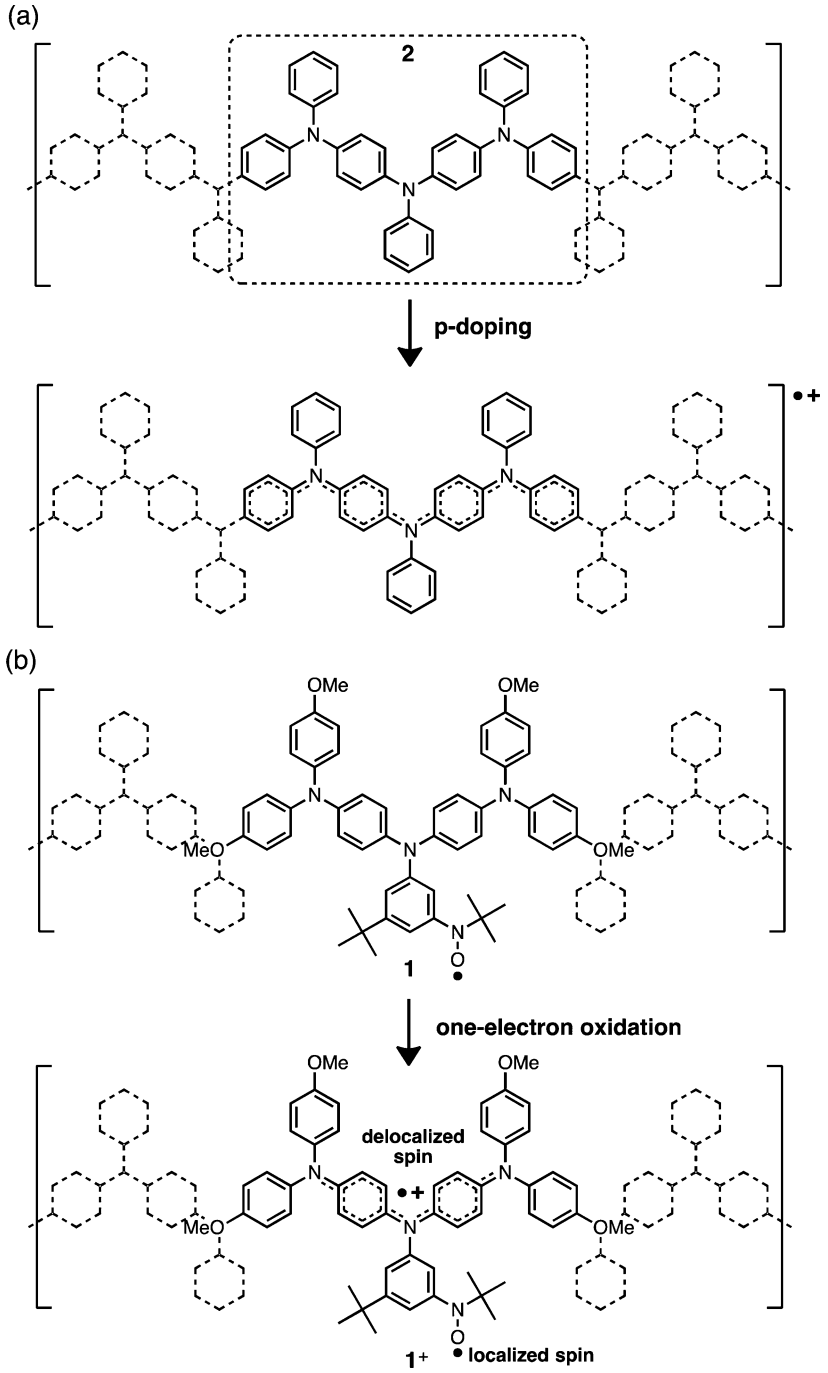

Figure 1. (a) *p*-Phenylene-linked oligoarylamine (triamine **2** as an example) and its delocalized polaronic state generated by p-type doping. (b) Niroxide-substituted triarylamine **1** embedded in the oligoarylamine molecular wire and its diradical cationic form, $\mathbf{1}^{+}$, as a minimal model toward spin-polarized molecular wires.

synthesized by using palladium-catalyzed amination reaction[14] of triamine **3**[15] with *tert*-butyldimethylsilyl-protected hydroxylamine **4**[16] (Scheme S1). The magnetic susceptibility measurement of prepared radical **1** was performed on a SQUID magnetometer from 300 to 2 K. The temperature dependence of the molar magnetic susceptibility (χ_M) of **1** was recorded at a constant field of 500 G. The plot of $\chi_M T$ versus T is shown in Figure S1. The $\chi_M T$ value of **1** in the temperature region above 30 K was very close to the theoretical value of 0.375 emu K mol^{-1} for an isolated spin of $^1/_2$, thus indicating the high purity of **1**. The EPR spectrum of **1** in toluene (T = 298 K) displayed a hyperfine structure consisting of a triplet of quartets originating from the hyperfine interaction with a single nitrogen nucleus (I = 1) and three magnetically equivalent aromatic hydrogen nuclei (I = $^1/_2$) at *ortho* and *para* positions to the substituted nitroxide group (Figure 2). From the spectral simulation, the hyperfine coupling constants were determined: $|a_N|$ = 1.25 mT (1N), and $|a_{H(ortho,para)}|$ = 0.19 mT (3H). In addition, an anisotropic EPR spectrum characteristic of nitroxide radical was detected in a frozen solution (Figure S2).[17] The observed spectrum supports the possibility that the spin is localized on the nitroxide moiety of **1**.

As revealed by cyclic voltammetry, **1** undergoes two reversible one-electron oxidations at −0.07 and +0.20 V and

DOI: 10.1021/acs.joc.6b02037
J. Org. Chem. 2016, 81, 11416−11420

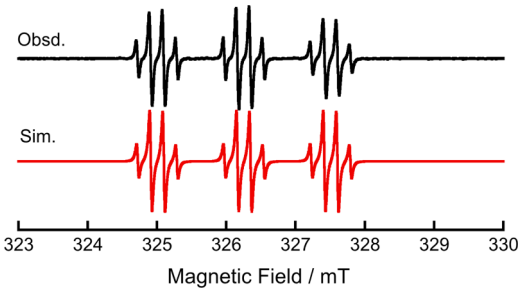

Figure 2. Observed and simulated X-band EPR spectra of **1** recorded in toluene at 298 K.

one irreversible oxidation with a peak potential of +0.55 V [vs $Fc^{0/+}$ (Figure S3)], thus indicating the formation of $\mathbf{1}^{+}$ and $\mathbf{1}^{2+}$ as stable oxidized species. Judging from the observation that triamine **3** (Scheme S1) exhibited two reversible one-electron oxidations at −0.18 and +0.11 V, while *N*-phenyl-*N*-*tert*-butyl nitroxide exhibited one irreversible oxidation with a peak potential of +0.41 V under the same conditions,[4b] it can be safely said that the first and second oxidation processes correspond to the removal of the first and second electrons, respectively, from the triamine moiety of **1**, while the third oxidation process corresponds to the oxidation of the nitroxide group. This observation can be rationalized by density functional theory (DFT) calculations of **1**. As shown in Figure 3, the relative energy levels of the frontier Kohn−Sham orbitals

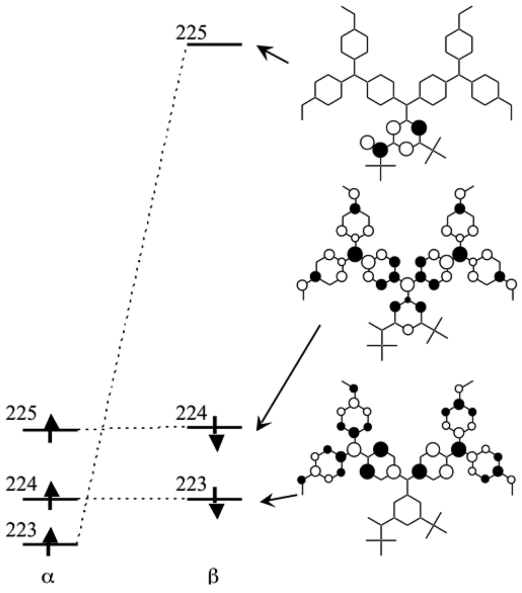

Figure 3. Relative energy levels of the frontier Kohn−Sham orbitals for **1** based on the UB3LYP/3-21G calculations.

calculated on the unrestricted B3LYP/3-21G level of theory clearly show the stabilization of α-HOMO-2 (223α) and the destabilization of β-LUMO (225β), which are both localized on the nitroxide groups, due to spin polarization. Thus, one-electron oxidation of **1** takes place by removal of an electron from β-HOMO (224β), which is distributed over the entire triamine moiety.

To confirm the delocalized polaronic state in $\mathbf{1}^{+}$ and the charge distribution of $\mathbf{1}^{2+}$, we measured the optical absorption spectral changes of **1** in CH_2Cl_2 during the course of the oxidation going from neutral **1** through monocation $\mathbf{1}^{+}$ to dication $\mathbf{1}^{2+}$ by using an optically transparent thin-layer electrochemical cell. During the oxidation of **1** to $\mathbf{1}^{+}$, new absorption bands appeared at 7257 cm^{-1} (0.90 eV, 1378 nm) and 12990 cm^{-1} (1.61 eV, 770 nm) (Figure 4). This spectral

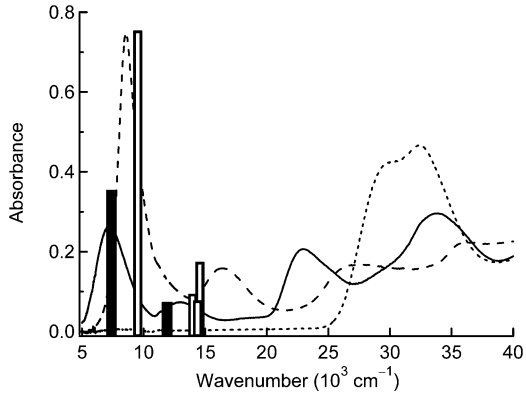

Figure 4. UV/vis/NIR spectra of **1** (···), $\mathbf{1}^{+}$ (—), and $\mathbf{1}^{2+}$ (---) in dichloromethane and 0.1 M *n*-Bu_4NBF_4. The black and white bars represent the TD-DFT-computed lowest and next lowest transition energies and their relative oscillator strengths for the triplet state of $\mathbf{1}^{+}$ and the doublet state of $\mathbf{1}^{2+}$, respectively.

pattern is quite similar to that reported for the radical cation of the closely related triamine {*N*,*N*-bis[4-(diphenylamino)-phenyl]-*N*-phenylamine},[6] which exhibited the charge-delocalized intervalence (IV) state. In fact, the time-dependent density functional theory (TD-DFT) results for the optimized structure of the triplet state of $\mathbf{1}^{+}$ elucidated the observed spectrum of $\mathbf{1}^{+}$ (Figure 4, FigureS4, and Table S1).[18] The lowest-energy band was ascribed mainly to the transition [7284 cm^{-1} (f = 0.56)] from β-HOMO (223β) to β-LUMO (224β) (67%). In addition, the next-lowest transition was mainly composed of the transition [12010 cm^{-1} (f = 0.14)] from β-HOMO-1 (222β) to β-LUMO (224β) (90%). The frontier orbitals associated with these transitions are distributed mainly over the triamine moiety and, hence, the observed lowest and next lowest transitions considered as charge resonance in a charge-delocalized state.[19] Moreover, the relative intensity between the lowest and next lowest bands was well-reproduced by the calculated oscillator strengths (Figure 4). All these things make it clear that a delocalized polaronic state is generated on the triamine moiety of $\mathbf{1}^{+}$. As shown in Figure 4, when $\mathbf{1}^{+}$ is further oxidized to $\mathbf{1}^{2+}$, the lowest and next lowest energy band observed for $\mathbf{1}^{+}$ were changed into more intense bands at 8620 cm^{-1} (1.07 eV, 1160 nm) and 16450 cm^{-1} (2.04 eV, 608 nm) with a hypsochromic shift, respectively. The origin of these electronic transitions could again be explained by TD-DFT calculations at the optimized structure for the doublet state of $\mathbf{1}^{2+}$, where the doubly positive charge is distributed mainly on the peripheral triarylamine moieties to avoid the electrostatic repulsion between two positive charges;[6] the lowest-energy band was rationalized as the charge resonance within the triamine moiety (Figure S5 and Table S1).

To ascertain the magnetic interaction between the localized spin on the nitroxide group and the delocalized spin generated on the triamine moiety of **1**, we measured the continuous wave (cw) EPR spectra at X-band frequencies in a frozen solution of $\mathbf{1}^{+}$, which was prepared by treatment with up to 1 molar equivalent of tris(4-bromophenyl)aminium hexachloroantimonate (Magic Blue)[20] in *n*-butyronitrile under an inert

DOI: 10.1021/acs.joc.6b02037
J. Org. Chem. 2016, 81, 11416−11420

atmosphere at 123 K. The observed spectrum of 1^+ had a poorly resolved fine structure in the spin-allowed resonance region, and furthermore, the spin-forbidden resonance at half-field, characteristic of a triplet state, was clearly detected (Figure 5a). Figure 5b shows the temperature dependence of the

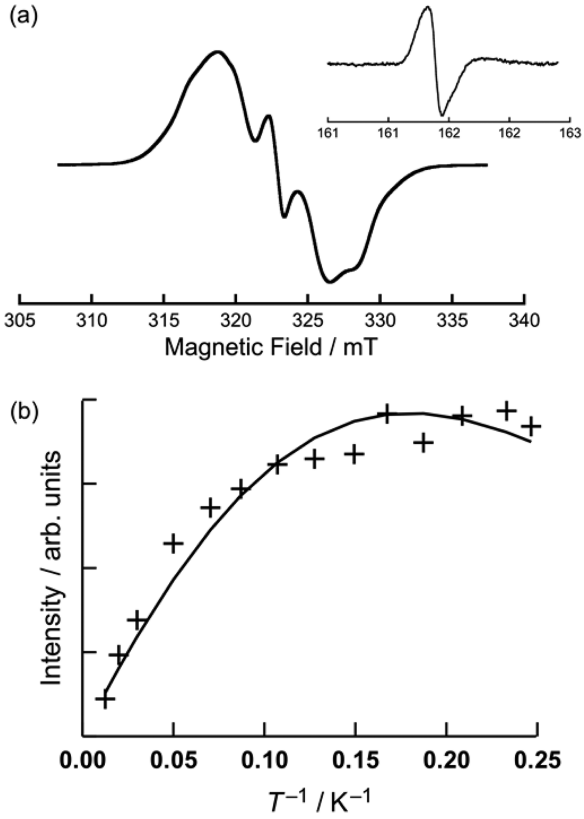

Figure 5. (a) X-Band EPR spectrum of 1^+ in *n*-butyronitrile at 123 K. The central signal is due to some doublet impurity. The inset shows the spin-forbidden resonance signal at half-field. (b) Plot of the observed spin-forbidden EPR signal intensity vs T^{-1} and the best theoretical fit to that data (—) (see the text).

doubly integrated EPR intensity (I) for the spin-forbidden signal of 1^+ as a function of the reciprocal temperature ($1/T$) between 4 and 80 K. The data were fit according to the singlet−triplet model (eq 1):[21]

$$I = \frac{C}{T}\frac{1}{3 + \exp\left(-\frac{\Delta E_{S-T}}{k_B T}\right)} \quad (1)$$

where C is the Curie constant and k_B the Boltzmann constant. The fit parameters give an energy gap between the singlet and triplet states (ΔE_{S-T}) of −17.6 cal mol^{-1}; that is, the localized and delocalized spins are weakly antiferromagnetically coupled. On the other hand, the DFT-computed energy gap for 1^+ was estimated to be +444 cal mol^{-1}. The discrepancy between experimental and theoretical results can be ascribed to the fact that the electron correlation, in particular, the static correlation, for the singlet state of 1^+ is not adequately taken into consideration at the UB3LYP level of theory, and hence, further theoretical consideration of this discrepancy is needed.[22] Upon further oxidation of 1^+ to 1^{2+}, the EPR spectrum in a frozen *n*-butyronitrile solution was very similar to that for **1** in a frozen toluene solution (Figure S6), indicating that the second oxidation leads to the doubly charged closed-shell electronic structure in the triamine moiety, leaving the localized spin on the nitroxide substituent intact.

In summary, we synthesized an oligoarylamine **1** bearing a nitroxide substituent as a localized spin center, where the nitroxide group is introduced at the central N position of the triamine moiety so as to interact magnetically with the delocalized polaronic spin that can be generated on the triamine moiety by one-electron oxidation of **1**. This result is a clear indication of the coexistence of both localized and delocalized spins in a single molecule, 1^+. Moreover, the intramolecular magnetic interaction between the two kinds of spin centers turned out to be weakly antiferromagntic. This work is expected to furnish new multispin molecular systems in which localized and delocalized spin centers are coexistent.

EXPERIMENTAL SECTION

General. *N,N*-Bis[4-(di-4-anisylamino)phenyl]amine **3**[15] and *N*-(3-bromo-5-*tert*-butylphenyl)-*N*-(*tert*-butyldimethylsiloxy)-*N*-*tert*-butylamine **4**[16] were prepared using literature procedures. Commercially available reagents were used as supplied. Solvents were purified, dried, and degassed following standard procedures. Compound numbering is shown in Scheme S1.

Synthesis. *N,N-Bis[4-(di-4-anisylamino)phenyl]-N-{3-tert-butyl-5-[N-(tert-butyldimethylsiloxy)-N-tert-butylamino]phenyl}amine (**5**).* A mixure of **3** (0.45 g, 0.73 mmol), **4** (0.30 g, 0.73 mmol), NaO^{t}Bu (175 mg, 1.82 mmol), Pd(dba)$_2$ (13.8 mg, 0.024 mmol), and 2-(di-*tert*-butylphosphino)biphenyl (14.3 mg, 0.048 mmol) was heated at 80 °C for 25 h while being stirred in toluene (8 mL) under an Ar atmosphere. After cooling, the reaction mixture was washed with a saturated aqueous $NaHCO_3$ solution. The resulting organic solution was dried over Na_2SO_4. After the evacuation of toluene, the remaining mixture was column-chromatographed on silica gel (eluent, 1:1 CH_2Cl_2/*n*-hexane) to afford **5** (570 mg, 82%) as a white solid: ^{1}H NMR (400 MHz, acetone-d_6) δ 6.88 (m, 27H), 3.77 (s, 12H), 1.24 (s, 9H), 1.08 (s, 9H), 0.89 (s, 9H), −0.08 (br s, 6H); ^{13}C NMR (100 MHz, acetone-d_6) δ 156.4, 152.2, 151.4, 147.8, 144.5, 142.5, 142.0, 126.4, 125.4, 123.2, 117.8, 117.3, 115.6, 115.4, 61.4, 55.6, 35.2, 31.5, 26.6, 26.5, 18.6, −4.3. Anal. Calcd for $C_{60}H_{72}N_4O_5Si$: C, 75.28; H, 7.58; N, 5.85. Found: C, 75.47; H, 7.57; N, 5.83.

*N,N-Bis[4-(di-4-anisylamino)phenyl]-N-[3-tert-butyl-5-(N-tert-butyl-N-oxylamino)phenyl]amine (**1**).* To an ice-cooled THF solution (4 mL) of **5** (300 mg, 0.31 mmol) was slowly added 1.55 mL (0.55 mmol) of a 1.0 M THF solution of tetrabutylammonium fluoride (TBAF). Stirring was continued for 45 min at ∼0 °C and, moreover, for 75 min at room temperature. After addition of water and Et_2O, the organic layer was separated, and the aqueous layer was extracted with Et_2O. The combined organic layer was dried over Na_2SO_4. The solvent was evaporated to dryness to afford 274 mg (∼100%) of a deep greenish solid, **6**, and the crude product was used without further purification. To an Et_2O solution (10 mL) of crude **6** was added an excess of Ag_2O (1.13 g, 4.87 mmol), and the reaction mixture was stirred for 4 h. After filtration through Celite, the solvent was evaporated under reduced pressure. The residue was chromatographed on basic alumina (eluent, 5:1 *n*-hexane/ethyl acetate) to give **1** (212 mg, 80%) as a brown solid: EPR (toluene at room temperature) g = 2.0061, $|a_N|$ = 1.25 mT, $|a_{H(ortho,para)}|$ = 0.19 mT; FABMS (3-NBA) m/z (relative intensity in percent) calcd for $C_{54}H_{58}N_4O_5$ $[M + H]^+$ 842, found 842 (37). Anal. Calcd for $C_{54}H_{57}N_4O_5$: C, 77.02; H, 6.82; N, 6.65; O, 9.50. Found: C, 77.06; H, 6.86; N, 6.58; O, 9.26.

Computational Methods. Geometry optimizations were conducted at the DFT UB3LYP/3-21G level of theory. Stationary points were determined by harmonic vibrational frequency analysis. TD-DFT calculations were performed at the UB3LYP/3-21G level at the UB3LYP/3-21G optimized geometries. All calculations were performed with Gaussian 03, version C.02.

DOI: 10.1021/acs.joc.6b02037
J. Org. Chem. 2016, 81, 11416−11420

■ ASSOCIATED CONTENT

Supporting Information

The Supporting Information is available free of charge on the ACS Publications website at DOI: 10.1021/acs.joc.6b02037.

SQUID data for **1** (PDF)

^{1}H and ^{13}C NMR spectra of compound **5**, EPR spectra of **1** and $\mathbf{1}^{2+}$, and additional DFT calculation results (PDF)

■ AUTHOR INFORMATION

Corresponding Author

*E-mail: aito@scl.kyoto-u.ac.jp.

Present Address

†Y.H.: Department of Chemistry, Graduate School of Science, Osaka University, Toyonaka, Osaka 560-0043, Japan.

Notes

The authors declare no competing financial interest.

■ ACKNOWLEDGMENTS

This work was partly supported by a Grant-in-aid for Scientific Research on Innovative Areas "New Polymeric Materials Based on Element-Blocks (No. 2401)" (JSPS KAKENHI Grant JP15H00734). Numerical calculations were partly performed at the Research Center for Computational Science in Okazaki, Japan.

■ REFERENCES

(1) (a) Sanvito, S. *Chem. Soc. Rev.* **2011**, *40*, 3336−3355. (b) Nakazaki, J.; Chung, I.; Matsushita, M. M.; Sugawara, T.; Watanabe, R.; Izuoka, A.; Kawada, Y. *J. Mater. Chem.* **2003**, *13*, 1011−1022. (c) Sugawara, T.; Matsushita, M. M. *J. Mater. Chem.* **2009**, *19*, 1738−1753. (d) Sugawara, T.; Komatsu, H.; Suzuki, K. *Chem. Soc. Rev.* **2011**, *40*, 3105−3118.

(2) (a) Jahn, B. O.; Ottosson, H.; Galperin, M.; Fransson, J. *ACS Nano* **2013**, *7*, 1064−1071. (b) Shil, S.; Bhattacharya, D.; Misra, A.; Klein, D. J. *Phys. Chem. Chem. Phys.* **2015**, *17*, 23378−23383. (c) Tsuji, Y.; Hoffmann, R.; Strange, M.; Solomon, G. C. *Proc. Natl. Acad. Sci. U. S. A.* **2016**, *113*, E413−E419.

(3) Ito, A.; Urabe, M.; Tanaka, K. *Polyhedron* **2003**, *22*, 1829−1836.

(4) (a) Ito, A.; Kurata, R.; Sakamaki, D.; Yano, S.; Kono, Y.; Nakano, Y.; Furukawa, K.; Kato, T.; Tanaka, K. *J. Phys. Chem. A* **2013**, *117*, 12858−12867. (b) Ito, A.; Nakano, Y.; Urabe, M.; Kato, T.; Tanaka, K. *J. Am. Chem. Soc.* **2006**, *128*, 2948−2953.

(5) (a) Hankache, J.; Wenger, O. S. *Chem. Rev.* **2011**, *111*, 5138−5178. (b) Heckmann, A.; Lambert, C. *Angew. Chem., Int. Ed.* **2012**, *51*, 326−392.

(6) Hirao, Y.; Ito, A.; Tanaka, K. *J. Phys. Chem. A* **2007**, *111*, 2951−2956.

(7) Ito, A.; Yokoyama, Y.; Aihara, R.; Fukui, K.; Eguchi, S.; Shizu, K.; Sato, T.; Tanaka, K. *Angew. Chem., Int. Ed.* **2010**, *49*, 8205−8208.

(8) Ito, A.; Sakamaki, D.; Ichikawa, Y.; Tanaka, K. *Chem. Mater.* **2011**, *23*, 841−850.

(9) (a) Demeter, D.; Jeux, V.; Leriche, P.; Blanchard, P.; Olivier, Y.; Cornil, J.; Po, R.; Roncali, J. *Adv. Funct. Mater.* **2013**, *23*, 4854−4861. (b) Mohamed, S.; Demeter, D.; Laffitte, J.-A.; Blanchard, P.; Roncali, J. *Sci. Rep.* **2015**, *5*, 9031.

(10) (a) Hirata, S.; Sakai, Y.; Masui, K.; Tanaka, H.; Lee, S. Y.; Nomura, H.; Nakamura, N.; Yasumatsu, M.; Nakanotani, H.; Zhang, Q.; Shizu, K.; Miyazaki, H.; Adachi, C. *Nat. Mater.* **2014**, *14*, 330−336. (b) Taneda, M.; Shizu, K.; Tanaka, H.; Adachi, C. *Chem. Commun.* **2015**, *51*, 5028−5031. (c) Shizu, K.; Tanaka, H.; Uejima, M.; Sato, T.; Tanaka, K.; Kaji, H.; Adachi, C. *J. Phys. Chem. C* **2015**, *119*, 1291−1297.

(11) Ćirić-Marjanović, G. *Synth. Met.* **2013**, *177*, 1−47.

(12) In this study, we use the term "localized spin" as radical moieties in which the unpaired electron resides mainly on a few atoms: in the nitroxide group in **1**, the spin density is distributed mainly on the N and O atoms, and the spin delocalization is confined within the neighboring phenyl group at the most.

(13) (a) Di Piazza, E.; Merhi, A.; Norel, L.; Choua, S.; Turek, P.; Rigaut, S. *Inorg. Chem.* **2015**, *54*, 6347−6355. (b) Shil, S.; Herrmann, C. *Inorg. Chem.* **2015**, *54*, 11733−11740. (c) Souto, M.; Lloveras, V.; Vela, S.; Fumanal, M.; Ratera, I.; Veciana, J. *J. Phys. Chem. Lett.* **2016**, *7*, 2234−2239.

(14) (a) Surry, D. S.; Buchwald, S. L. *Angew. Chem., Int. Ed.* **2008**, *47*, 6338−6361. (b) Hartwig, J. F. *Nature* **2008**, *455*, 314−322. (c) Hartwig, J. F. *Acc. Chem. Res.* **2008**, *41*, 1534−1544.

(15) Hirao, Y.; Ino, H.; Ito, A.; Tanaka, K.; Kato, T. *J. Phys. Chem. A* **2006**, *110*, 4866−4872.

(16) Ishida, T.; Iwamura, H. *J. Am. Chem. Soc.* **1991**, *113*, 4238−4241.

(17) Griffith, O. H.; Waggoner, A. S. *Acc. Chem. Res.* **1969**, *2*, 17−24.

(18) The present diradical cation $\mathbf{1}^{+}$ exhibited a small energy gap between the singlet and triplet states (ΔE_{S-T}). This was also supported by the DFT calculations on $\mathbf{1}^{+}$. This means the singlet state should be considered for the assignment of the observed low-energy absorption bands (Figure 4). TD-DFT calculations for the open-shell singlet state resulted in transition energies similar to those for the triplet state: the lowest and next lowest transition energies were computed to be 7216 cm^{-1} (f = 0.51) and 12170 cm^{-1} (f = 0.12), respectively. The observed broad bands can be considered as a statistical superposition of the contribution from both spin states of $\mathbf{1}^{+}$ (see Table S1 for details).

(19) (a) Ishitani, A.; Nagakura, S. *Mol. Phys.* **1967**, *12*, 1−12. (b) Badger, B.; Brocklehurst, B.; Russell, R. D. *Chem. Phys. Lett.* **1967**, *1*, 122−124. (c) Szeghalmi, A. V.; Erdmann, M.; Engel, V.; Schmitt, M.; Amthor, S.; Kriegisch, V.; Nöll, G.; Stahl, R.; Lambert, C.; Leusser, D.; Stalke, D.; Zabel, M.; Popp, J. *J. Am. Chem. Soc.* **2004**, *126*, 7834−7845.

(20) (a) Bell, F. A.; Ledwith, A.; Sherrington, D. C. *J. Chem. Soc. C* **1969**, 2719−2720. (b) Connelly, N. G.; Geiger, W. E. *Chem. Rev.* **1996**, *96*, 877−910.

(21) Bleaney, B.; Bowers, K. D. *Proc. R. Soc. London, Ser. A* **1952**, *214*, 451−465.

(22) In addition, it was also pointed out that large dihedral angles between the *m*-phenylene π-face and the spin-bearing groups (60−90°) result in a preference for the spin-singlet ground state in diradicals; for $\mathbf{1}^{+}$, the dihedral angles of the *m*-phenylene π-face for the nitroxide group and the triamine moiety are estimated to be 0° and 47°, respectively, according to the present B3LYP/3-21G optimized structure (Figure S7). See, for example: (a) Kanno, F.; Inoue, K.; Koga, N.; Iwamura, H. *J. Am. Chem. Soc.* **1993**, *115*, 847−850. (b) Fang, S.; Lee, M.-S.; Hrovat, D. A.; Borden, W. T. *J. Am. Chem. Soc.* **1995**, *117*, 6727−6731.

DOI: 10.1021/acs.joc.6b02037
J. Org. Chem. 2016, 81, 11416−11420